

Review

Films and Materials Derived from Aminomalononitrile

Helmut Thissen¹, Richard A. Evans¹ and Vincent Ball^{2,3,*}

¹ CSIRO Manufacturing, Research Way, Clayton, VIC 3168, Australia; Helmut.thisse@csiro.au (H.T.); richard.evans@csiro.au (R.A.E.)

² Faculté de Chirurgie Dentaire, Université de Strasbourg, 8 rue Sainte Elisabeth, 67000 Strasbourg, France

³ Institut National de la Santé et de la Recherche Médicale, Unité Mixte de Recherche 1121, 11 rue Humann, CEDEX, 67085 Strasbourg, France

* Correspondence: vball@unistra.fr

Abstract: In recent years major advances in surface chemistry and surface functionalization have been performed through the development, most often inspired by living organisms, of versatile methodologies. Among those, the contact of substrates with aminomalononitrile (AMN) containing solutions at pH = 8.5 allows a conformal coating to be deposited on the surface of all known classes of material. Since AMN is a molecule probably formed in the early atmosphere of our planet and since HCN-based compounds have been detected on many comets and Titan (Saturn's largest moon) it is likely that such molecules will open a large avenue in surface functionalization mostly for bio-applications. This mini review describes the state of the art of AMN-based coatings from their deposition kinetics, composition, chemical reactivity, hypothetical structure to their first applications as biomaterials. Finally, the AMN-based versatile coatings are compared to other kinds of versatile coating based on catecholamines and polyphenols.

Keywords: aminomalononitrile; prebiotic chemistry; versatile coatings; biomaterials



Citation: Thissen, H.; Evans, R.A.; Ball, V. Films and Materials Derived from Aminomalononitrile. *Processes* **2021**, *9*, 82. <https://doi.org/10.3390/pr9010082>

Received: 25 November 2020

Accepted: 28 December 2020

Published: 1 January 2021

Publisher's Note: MDPI stays neutral with regard to jurisdictional claims in published maps and institutional affiliations.



Copyright: © 2021 by the authors. Licensee MDPI, Basel, Switzerland. This article is an open access article distributed under the terms and conditions of the Creative Commons Attribution (CC BY) license (<https://creativecommons.org/licenses/by/4.0/>).

1. Introduction

Questions about the origin of life on Earth started to be asked from a scientific point of view at the beginning of the 20th century. Besides the panspermia model in which the molecular building blocks of life are suspected to have an extra-terrestrial origin [1], theories emerged to describe the appearance of molecules able to yield building blocks of biomolecules from the chemical species present in the primitive atmosphere. This atmosphere, believed to be reductive, was also submitted to high energy conditions like spark discharges, volcanic eruptions and so on. In such conditions, the experiment performed by Stanley Miller showed the possibility to form amino acids, principally glycine, and some nucleobases [2,3]. These building blocks of proteins and nucleotides can also be formed from HCN and other cyano compounds [4–6]. Among oligomers of HCN, the dimers (iminoacetonitrile), trimer (aminomalononitrile) and tetramer (diaminomaleonitrile) can indeed yield complex polymeric species under certain physicochemical conditions [7,8]. In addition, evidence for the presence of some HCN-derived materials has been found on a broad range of comets as well as on Titan, Saturn's largest moon [9]. Besides these fundamental questions, some studies, summarized in [10], suggest the possible use of those molecules in materials science. In particular, the HCN trimer, aminomalononitrile (AMN), has been demonstrated to polymerize spontaneously in slightly alkaline conditions and at ambient temperature, leading not only to the precipitation of a brown-reddish precipitate but also to a conformal coating on almost all known classes of material [11]. It is the aim of this mini-review to summarize the knowledge acquired about these coatings and to describe their possible applications in biomedical applications and environmental science. Finally, we compare AMN based coatings with other universal coatings such as those based on the oxidative polymerization/self-assembly of catecholamines.

2. Film Deposition and Characterization

2.1. Film Deposition and Kinetic Aspects

When substrates as different as polymers, metals and ceramics are put in AMN solutions at pH = 8.5, this leads to the neutralization of the p-toluenesulfonate salt, and the formation of a coating with a brown colour (inset in Figure 1). The deposition kinetics is, however, relatively slow, with an average growth rate of about $3.8 \text{ nm}\cdot\text{h}^{-1}$ from a 2% (*w/v*) AMN solution as determined by atomic force microscopy [11]. By focusing on shorter deposition times, it was shown that the film deposition is preceded by an AMN concentration dependent lag phase (Figure 1) whereas the reaction in solution starts from $t = 0$ on, corresponding to the pH adjustment to 8.5 [12]. The occurrence of a monomer-dependent lag phase may be an indication of a heterogeneous nucleation process preceding film deposition.

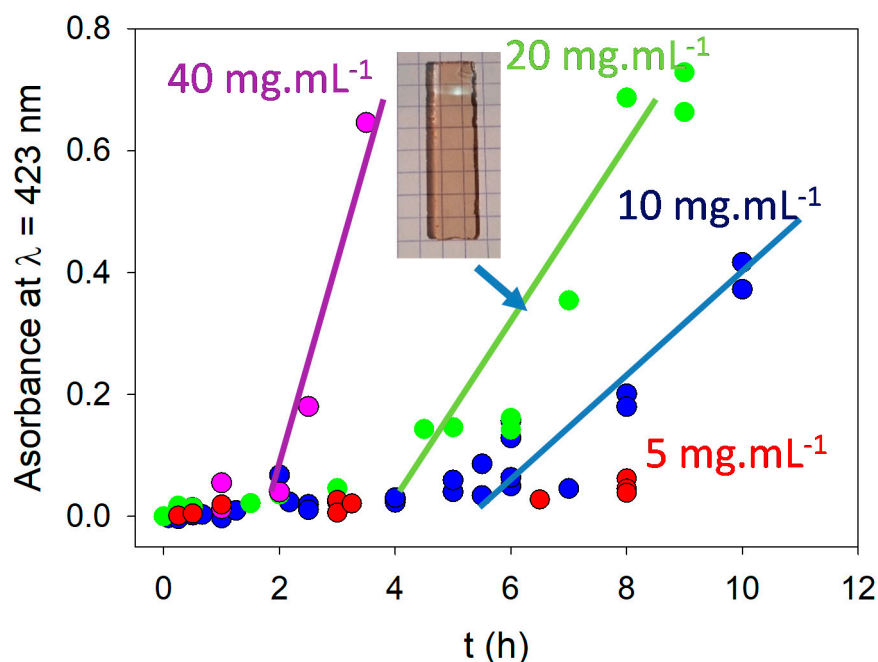


Figure 1. Absorbance at $\lambda = 423 \text{ nm}$ of aminomalonnitrile (AMN)-based films deposited on quartz slides at different concentrations of AMN: 5 (\bullet), 10 (\bullet), 20 (\bullet) and 40 (\bullet) $\text{mg}\cdot\text{mL}^{-1}$. The lines are aimed to guide the eye and their extrapolation to the time axis yields the induction period preceding the deposition of the AMN based films. The inset is a picture of a quartz slide after 8 h of deposition from a $20 \text{ mg}\cdot\text{mL}^{-1}$ AMN solution. Reproduced with permission from [12], Copyright American Chemical Society, 2019.

The film deposition can be accelerated, in the presence of 2,3-dihydroxybenzaldehyde or in the presence of 2,3,4-trihydroxybenzaldehyde (Figure 2). The effective incorporation of these building blocks has been demonstrated by means of X-ray photoelectron spectroscopy (XPS) by a reduction of the N/C ratio in comparison to coatings obtained in the presence of AMN only [12]. Hence, not only the kinetics of film deposition but also its composition are affected by the addition of 2,3-dihydroxybenzaldehyde or 2,3,4-trihydroxybenzaldehyde in the reaction mixture.

2.2. Film Morphology and Hydrophilicity

The film morphology on polystyrene substrates was strongly dependent on the concentration of the phosphate buffer at a constant pH of 8.5, changing from a needle-like to a grainy morphology upon a decrease in phosphate buffer concentration from 100 mM to 0 mM [11]. For a given concentration in phosphate buffer, the film morphology obtained on glass substrates was also time dependent with a transition from islands to fibres (Figure 3).

The formation of fibres in the absence of templating agents is intriguing and points to the occurrence of direction-specific interactions.

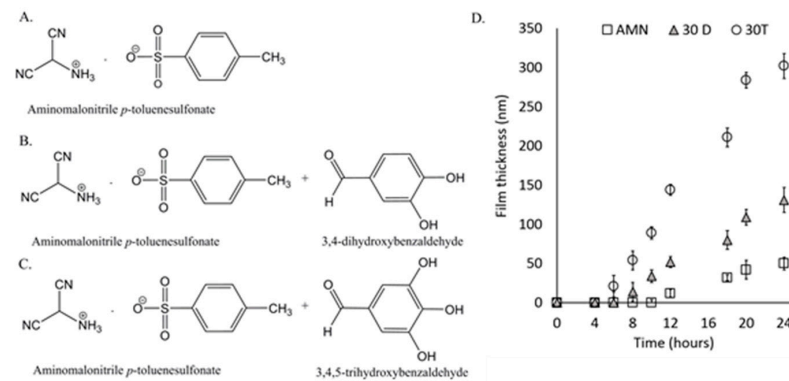


Figure 2. Structure of the parabenzenesulfonate salt of AMN (A). Addition of benzaldehydes: dihydroxybenzaldehyde (B) and 2,3,4-trihydroxybenzaldehyde (C) and the coating thickness achieved over time using these components (D). Here, AMN refers to 100 mol% aminomalononitrile, while 30D refers to 30 mol% 2,3-dihydroxybenzaldehyde and 70 mol% aminomalononitrile and 30T refers to 30 mol% 2,3,4-trihydroxybenzaldehyde and 70 mol% aminomalononitrile. Reproduced with permission from [13], Copyright American Chemical Society, 2017.

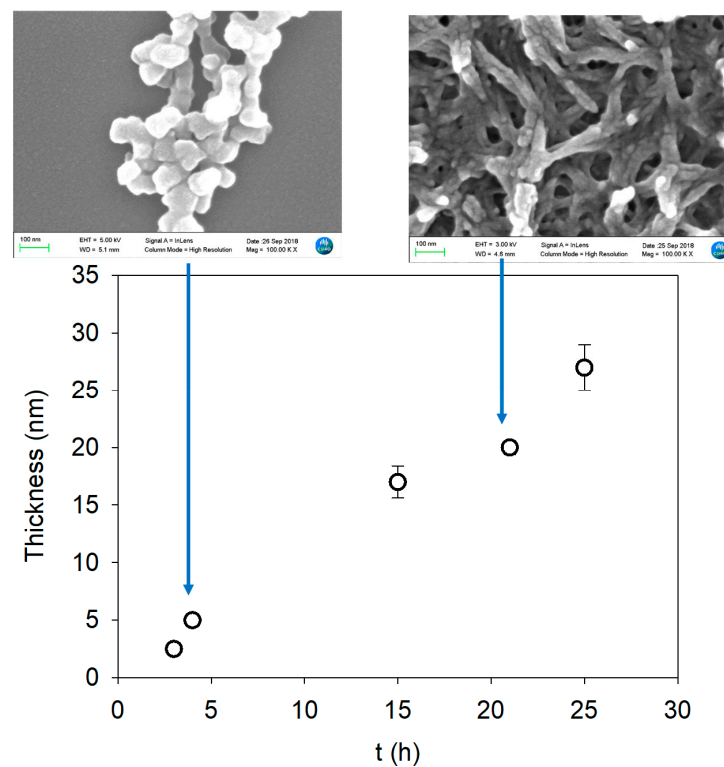


Figure 3. Morphologies of AMN based films obtained by scanning electron microscopy (SEM) after 4.5 h and 21 h of deposition are shown in the upper part and related to the deposition kinetics (lower part) measured by means of single wavelength (632.8 nm) ellipsometry. The deposition was performed using a $10 \text{ mg} \cdot \text{mL}^{-1}$ AMN solution in the presence of 50 mM phosphate buffer at $\text{pH} = 8.5$. The scale bar corresponds to 100 nm in each micrograph. The full image size is about $1 \mu\text{m} \times 1 \mu\text{m}$. Reproduced with permission from [14], Copyright Elsevier, 2020.

In all cases, the obtained coatings seem however to be conformal and pinhole free. This was also confirmed by electrochemistry and in particular by means of electrochemical

impedance spectroscopy [12] as well as by XPS, where the photoelectrons corresponding to Si disappear progressively upon AMN film deposition.

2.3. Film Composition and Structure

AMN films, prepared from 2% (*w/v*) aqueous solutions, were found by XPS to have an N/C ratio of 0.61 ± 0.02 which was independent from the substrate material (polymers, even poly(tetrafluoroethylene), gold, glass and mica) used in the experiments [11]. The investigation of the film composition with deposition time on silicon oxide slides showed a progressive disappearance of the Si2p and Si2s photoelectrons demonstrating the formation of a conformal and pinhole-free coating. The steady state N/C ratio close to 0.6 is reached only after a prolonged time, while during the first 4 h of the deposition process in the presence of $10 \text{ mg}\cdot\text{mL}^{-1}$ AMN, almost no N is detected on the surface in agreement with the occurrence of a lag phase (Figure 1) preceding film deposition. AMN itself is characterized by a N/C ratio of 1 (see its structure in Figure 2). Film deposition experiments performed on gold substrates have suggested that some cyanide anions are released during the chemical reaction in alkaline conditions [12]. This release of CN^- , however, does not allow to explain the finding that the coatings, even if they are nitrogen rich, display a N/C ratio significantly lower than 1. We made the assumption that some hydrolysis of imine groups present in the coating will lead to the formation of carbonyls and a loss of nitrogen. The possible occurrence of such a hydrolysis step is also consistent with the presence of O in the composition of the films (Figure 4, this O being not due to the substrate owing to the lack of the Si2p and Si2s photoelectrons). Aminomalononitrile is a highly functionalized molecule that contains two different nucleophilic centres ($-\text{NH}_2$ and $\text{R}-\text{C}-\text{H}$) and two electrophilic centres ($-\text{CN}$) and many mechanisms of polymerization and polymeric structures can be proposed. A hypothetical structure of the AMN-based film is represented in Scheme 1 to illustrate how N/C and O/C ratios of 0.66 and 0.33, respectively, might be obtained.

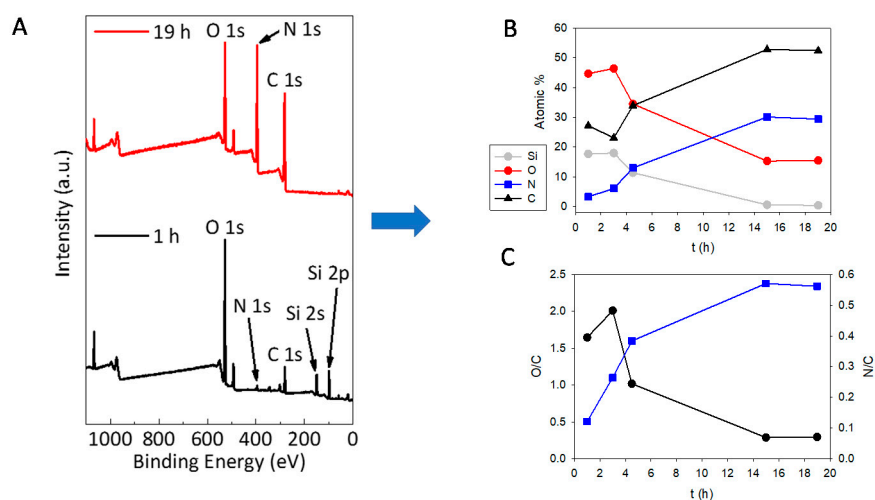
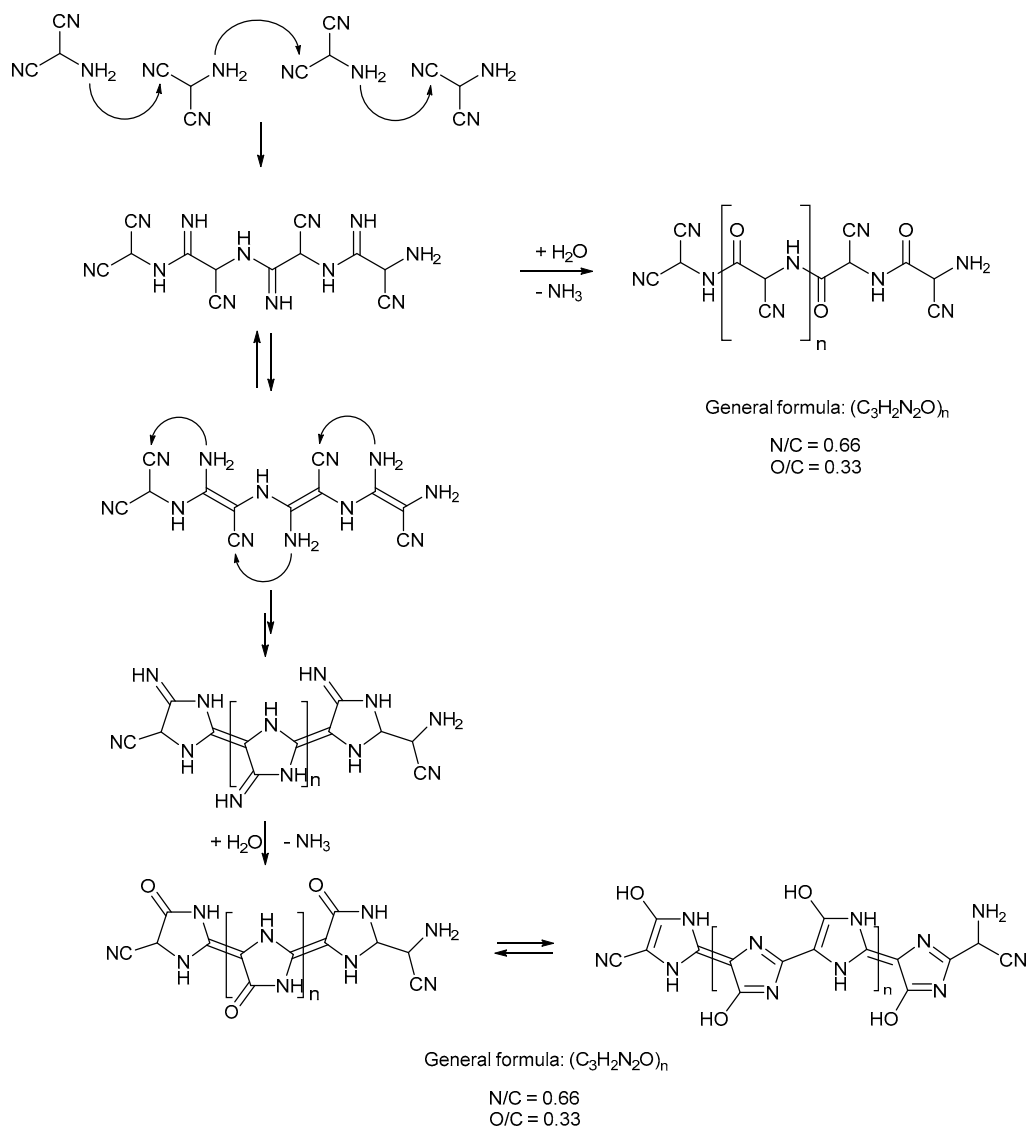


Figure 4. (A) X-ray photoelectron spectroscopy (XPS) survey spectra of AMN-based films after different deposition times (1 h and 19 h) on glass slides. (B) Evolution of the atomic percentage of Si (●), O (●), N (■) and C (▲) as a function of time for AMN based coatings deposited from a $10 \text{ mg}\cdot\text{mL}^{-1}$ solution. The coatings were deposited on Si containing glass slides. (C) Evolution of the O/C (●) and N/C (■) ratios with reaction time in a $10 \text{ mg}\cdot\text{mL}^{-1}$ AMN solution. The error bars correspond to \pm one standard deviation. Reproduced with permission from [12], Copyright American Chemical Society, 2019.



Scheme 1. A possible structure of the polymeric material obtained at the solid-liquid interface from an AMN based solution at pH = 8.6, and the different steps leading to an O containing film and with the observed N/C and O/C ratios.

Note that many tautomeric structures are possible and we have illustrated just two. The given atomic ratios are obtained by the addition of water and loss of ammonia in every AMN repeat unit.

The possible presence of heteroaromatic monomers in the obtained material is consistent with the formation of fibres (Figure 2) during the deposition process since such structural building blocks may interact through directional π - π stacking. Note that the structure we propose for our AMN-based materials are similar to those characterized from other HCN-derived polymers and materials [15].

2.4. Chemical Reactivity of the Aminomalonnitrile (AMN)-Based Films

2.4.1. Reactivity with Trifluoroacetaldehyde Ethyl Hemiacetal (TFAEH) and with 4-Bromobenzylbromide (BBB)

Trifluoroacetaldehyde ethyl hemiacetal (TFAEH) was added to the AMN solutions or the obtained AMN films were treated with this fluorinated organic compound. The F/C ratio calculated by XPS showed that above a threshold concentration of about 10^{-3} M, fluorine incorporation increased with increasing concentration of the fluorinated co-monomer [11]. The efficiency of fluorine incorporation was much higher in the co-deposition than in the post-deposition experiment. This experiment demonstrates that the AMN based coat-

ings contain some nucleophilic groups. When AMN is reacted with the electrophilic 4-bromobenzylbromide (BBB), some bromide is also incorporated in the obtained film, as shown by XPS, confirming again the presence of electrophiles in the AMN-based material [11].

2.4.2. Reactivity with Ag^+ Cations

When an AMN-based film is put in silver nitrate solutions (concentrations from 1 to 100 mM), silver is detected in its ionic and metallic form by means of XPS. This shows the ability of the obtained films to coordinate silver cations. The presence of metallic silver was attributed either to the presence of reducing moieties or to the ability of the film to induce a disproportionation reaction [11]. The occurrence of an antioxidant activity of the AMN-based films was shown in a recent investigation [14].

2.4.3. Anti-Oxidant Properties

AMN-based films deposited on an amorphous carbon electrode from a solution at $\text{pH} = 8.5$ also display some oxidation current when the potential is cycled between -0.6 and $+1.0$ V versus the reference electrode in a cyclic voltammetry experiment [14]. This finding shows that AMN based films are able to reduce some chemicals in contact with them, and could also explain the possibility to obtain a metallic silver content when the film is exposed to a silver nitrate solution, as explained previously. To test this reducing ability with respect to organic molecules, the AMN-based films were put in contact with ethanolic solutions of 2,2-diphenyl-1-picrylhydrazyl (DPPH). When this radical species undergoes a reduction process it changes colour from purple to yellow which can be followed spectrophotometrically. Such a colour change is indeed found in the presence of AMN-based films obtained from solution deposition and shows the intrinsic antioxidant properties of these coatings (Figure 5A). The antioxidant activity first increases with the film thickness before saturation after about 15 h of film deposition (Figure 5B). However, the film thickness continues to increase even for longer deposition times, suggesting that the parts of the AMN film close to the film substrate interface are not accessible any more to the bulky DPPH [14].

2.5. Deposition of AMN-Based Films Using Cyclic Voltammetry

When an amorphous carbon working electrode is immersed in a $10 \text{ mg}\cdot\text{mL}^{-1}$ containing AMN solution at $\text{pH} = 6.0$, no film deposition occurs in the absence of potential cycling. However, when the potential is cycled between -0.7 and $+1.0$ V vs. the reference electrode, in a cyclic voltammetry experiment, an oxidation current is measured above 0 V vs. the reference electrode. This electrochemical phenomenon is irreversible since no faradaic reduction current is measured during the backward scan from $+1.0$ to -0.7 V [16]. The oxidation current then progressively decreases when additional potential sweep is performed (Figure 6A). This suggests the formation of a coating hindering further access of the AMN monomer to the surface of the working electrode. Indeed, the coating obtained becomes impermeable to potassium hexacyanoferrate after about 7 cyclic voltammetry cycles performed at a potential sweep rate of $50 \text{ mV}\cdot\text{s}^{-1}$ in the presence of AMN ($10 \text{ mg}\cdot\text{mL}^{-1}$ with 50 mM sodium phosphate buffer at $\text{pH} = 6.0$). In addition, this AMN-based coating displays by itself some electroactivity. It has also been shown that electrochemical properties of the AMN based coatings as their capacitance (as calculated from electrochemical impedance spectra) are dependent on the potential sweep rate at which the deposition by cyclic voltammetry is performed. This shows that the AMN-based film deposition requires some oxidation of the AMN monomers coupled with chemical processes defined by intrinsic rate constants. Such reaction mechanisms will have to be investigated in the future.

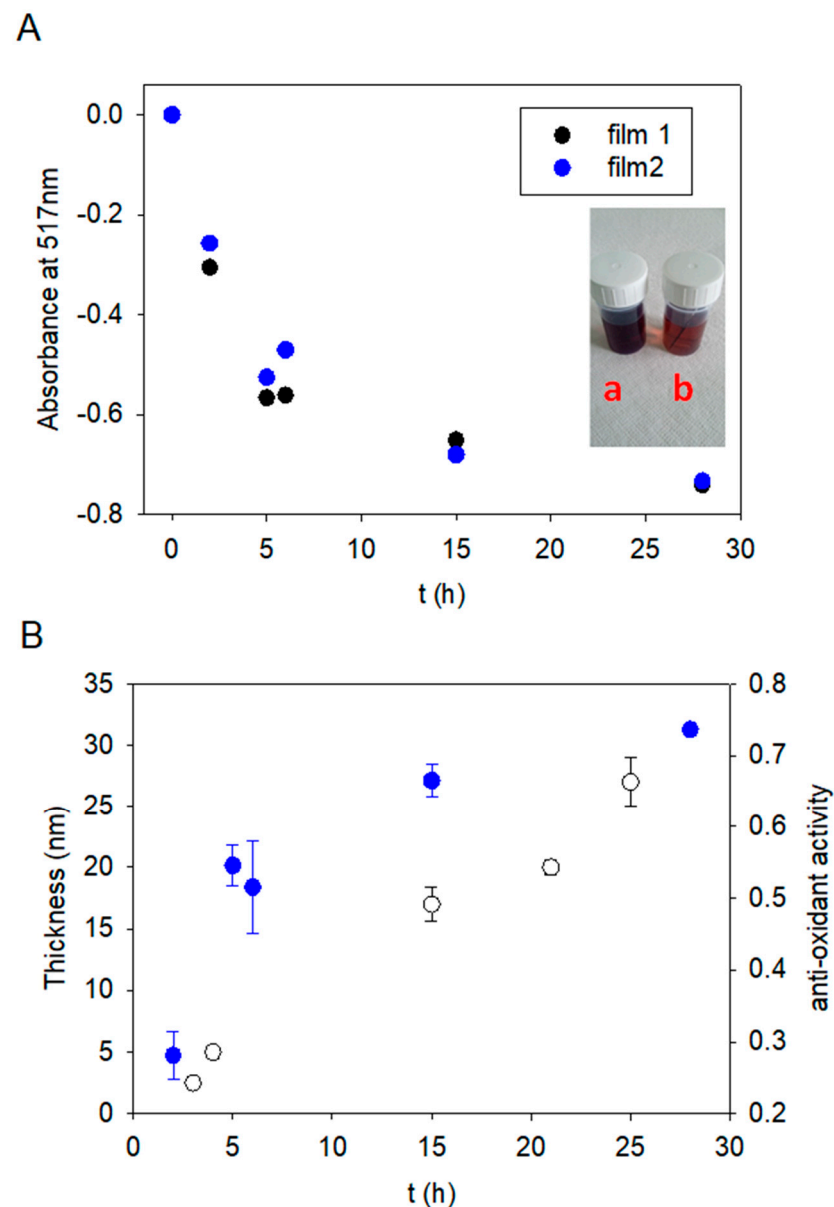


Figure 5. (A) Evolution of the absorbance at 517 nm of a 2,2-diphenyl-1-picrylhydrazyl (DPPH) solution (10^{-4} M in ethanol) put in contact for 30 min with an AMN film deposited on glass for the indicated duration. The picture corresponds to a DPPH solution kept in the dark (reference, picture a) and a DPPH solution kept in the dark but in contact with an AMN based film deposited for 5 h on a glass slide (picture b). 2 individual measurement series were performed (●,●). (B) Evolution with time of the AMN-based film thickness (same data as in Figure 1, left hand scale) and their anti-oxidant activity (taken as the average \pm one standard deviation (SD) from the data in part A, right hand scale). Reproduced with permission from [14], Copyright Elsevier, 2020.

XPS was used to determine the chemical composition of the AMN based films obtained after 10, 20 or 50 CV cycles (at a potential sweep rate of $50 \text{ mV}\cdot\text{s}^{-1}$). It came out that the films obtained through electrochemical deposition have a composition that is extremely close if not identical to the composition of the AMN-based film obtained from solution deposition at $\text{pH} = 8.5$ (Figure 6B). The possibility to obtain AMN-based films on conductive materials offers the possibility to coat materials in a controlled manner without loss of monomers in the form of precipitated materials which occurs when AMN polymerization is performed in solution at a sufficiently high pH value [11,12].

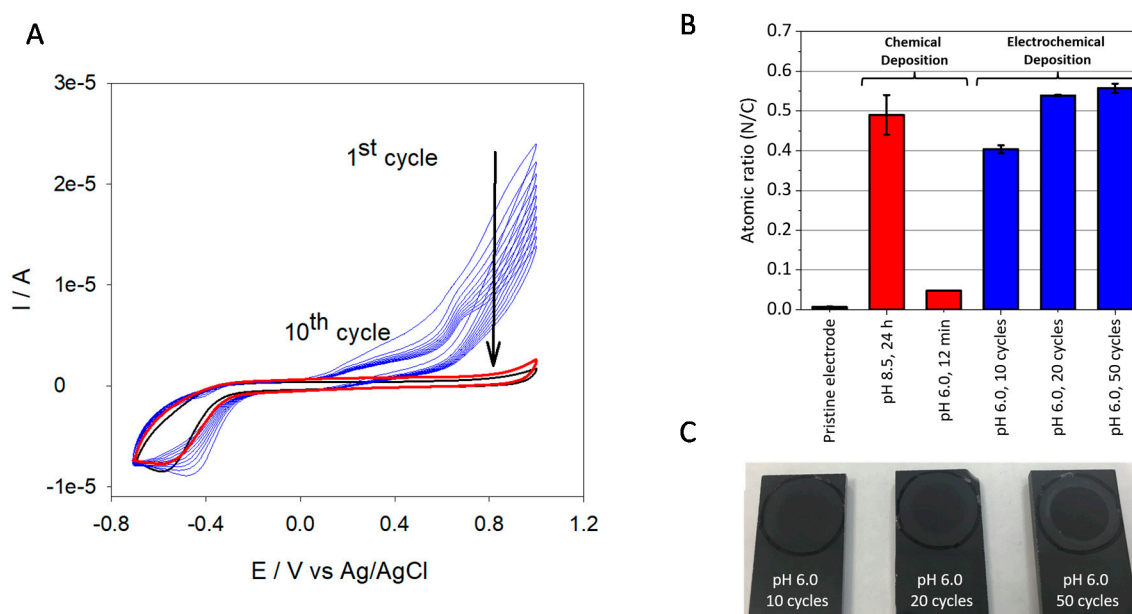


Figure 6. (A) A typical cyclic voltammetry experiment performed at $50 \text{ mV}\cdot\text{s}^{-1}$ in the presence of sodium phosphate buffer on the pristine amorphous carbon electrode (—) and on the electrode covered with an AMN-based film (—) after 10 CV cycles (performed at $50 \text{ mV}\cdot\text{s}^{-1}$) in the presence of AMN at $10 \text{ mg}\cdot\text{mL}^{-1}$ (—). The black vertical arrow indicates the evolution of the faradaic current from the first to the 10th CV cycle. (B) Average nitrogen-to-carbon (N/C) elemental ratios acquired from XPS spectra on pristine carbon electrode before and after chemical or electrochemical deposition of AMN-based films ($n = 3$, error bars represent one standard deviation; lines are drawn to guide the eye). All depositions was carried out in the presence of $10 \text{ mg}\cdot\text{mL}^{-1}$ AMN. Electrochemical deposition was performed with CV at a scan rate of $50 \text{ mV}\cdot\text{s}^{-1}$. (C) Appearance of AMN based films deposited with increasing number of CV sweep cycles. Reproduced with permission from [16], Copyright Elsevier, 2018.

3. Applications of AMN-Based Films

Because prebiotic chemistry is considered to have been important for the production of the molecules and macromolecules required for life to have arisen, it is surprising that this chemistry has not been examined in more detail for its compatibility with biology [11]. However, aminomalononitrile-based coatings and their copolymers have recently been shown to have high biocompatibility and an outstanding ability to support mammalian cell attachment [11,16]. Figure 7 shows an example where the attachment of L929 mouse fibroblasts was investigated on a tissue culture polystyrene (TCPS) control surface (a), as well as a commercially available ultra-low attachment surface (ULA, Corning) and an ULA surface coated with an AMN coating (c). After 24 h, cell attachment increased from 3% on the non-cell adherent ULA surface to 127% on the ULA-AMN surface relative to TCPS (d). After microarray contact printing of an AMN solution on the ULA surface, cell attachment was also found to be restricted to the AMN coated area (e). In addition, Figure 7 shows an example for a 24 h crystal violet biofilm assay on AMN coatings incubated with silver nitrate. The data obtained for the representative bacterial strains *S. epidermidis* (Gram-positive) and *P. aeruginosa* (gram negative) show a concentration dependent decrease in biofilm formation, with effective antimicrobial activity being achieved above silver nitrate concentrations of 10^{-5} M used for incubating the AMN coatings.

As the effective control over biointerfacial interactions is the key to a broad range of new and improved biomedical devices and related applications, surface coatings that are biocompatible while they are independent of the substrate material are of outstanding interest. Application examples that have been explored to date range from cell culture tools that are supportive for mammalian cell attachment [11] to coatings for bone-contacting applications where the utility of the coatings as osteogenic support matrices via the induced osteogenic differentiation of human mesenchymal stem cells (hMSCs) has been

reported [13]. Examples for AMN-based coatings with antimicrobial properties range from broad spectrum antimicrobial coatings preventing the formation of biofilms [11] to coatings for the removal of pathogens in stormwater [17]. Moreover, recently the copolymerisation of AMN polymer with a low biofouling polymer synthesized from sulfobetaine methacrylate and 2-aminoethyl methacrylate has been demonstrated to achieve the prevention of serum protein adsorption and cell attachment in vitro while also leading to a significant reduction in the foreign body response in nude mice in vivo over a period of 4 weeks [18]. Furthermore, the copolymerisation of AMN with low biofouling polymers was also exploited to achieve effective antimicrobial coatings [19]. Overall, these application examples demonstrate the advantages and the translational potential of this unique prebiotic chemistry-inspired surface modification strategy.

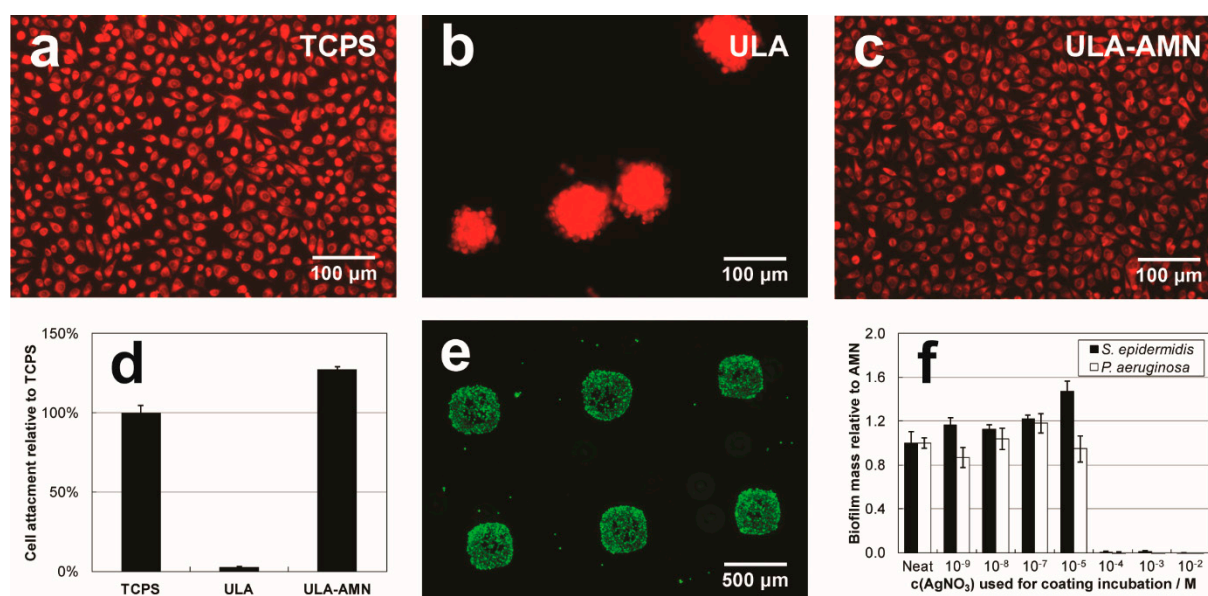


Figure 7. After 24 h cell culture, L929 mouse fibroblast cells show excellent attachment and spreading on tissue culture polystyrene (TCPS) control surfaces (a), while attachment is prevented on ultra-low attachment (ULA) control surfaces, leading to cell clumping (b). On AMN polymer coatings deposited on to ULA surfaces (ULA-AMN), cell attachment and spreading is equivalent to the TCPS surface, reversing the effect of the underlying ULA surface (c). The quantification of cell attachment via a cell proliferation assay supports these observations (d). Spatial control over L929 cell attachment was demonstrated on an ULA surface onto which an AMN solution was microarray contact printed (e). A 24 h crystal violet biofilm assay was used to demonstrate the effective antimicrobial activity of an AMN coatings that were incubated with different silver nitrate concentrations in contact with two representative bacterial strains, *S. epidermidis* and *P. aeruginosa* (f). Reproduced with permission from [11].

4. Analogies between Coatings Produced from AMN, Dopamine and Polyphenols

AMN-based films form conformal coatings with a substrate-independent N/C ratio on all classes of known material [11,12]. The related coating technology may hence be considered as versatile. Since similar versatile coating methodologies based on catecholamines [20] and polyphenols [21] have emerged in the last few years it is worth comparing these with AMN based coatings:

- (i) The kinetics of film deposition is slow, taking several hours to tens of hours. However, in the case of dopamine as a monomer unit, the formation of polydopamine may be considerably accelerated in the presence of strong oxidants like sodium periodate [22]. Even if oxidants could play a role in the deposition of AMN-based films, owing to a slight gradient in film deposition observed close to the water/air interface, it remains to be investigated how to speed up the deposition of AMN based films by other methods than the co-deposition in the presence of 3,4,5-trihydroxybenzaldehyde [16].

The AMN-based coatings seem to be differentiated from polydopamine coatings by the occurrence of a monomer concentration-dependent lag phase preceding film deposition [12].

- (ii) AMN-based films [12] and polydopamine like films [23] also spontaneously form at the water/air interface in the absence of shaking. This is related to the formation of amphiphilic species starting from highly water soluble monomers during the course of the polymerization process.
- (iii) The AMN-based coatings [14] and polydopamine films [24] contain some electroactive groups as evidenced by electrochemical methods and by discoloration of molecules like DPPH, related to the antioxidant activity of these coatings. The ability to reduce metal cations like Ag^+ is also related to the reducing power of those films. The same holds true for polyphenol-based films [21].
- (iv) All films produced either from AMN [11,13,18,19], dopamine [20], and a large set of polyphenols [21] are highly biocompatible. In fact, the application fields of PDA and AMN-based films are very similar even though the chemical pathways leading up to these coatings are different.

5. Conclusions

With an increasing understanding of the underlying mechanisms that govern the formation of prebiotic chemistry inspired aminomalononitrile based coatings and a rapidly increasing number of application examples, these coatings are expected to be translated into a range of applications, and in particular applications at the interface between biology and materials science, such as biomedical device applications. These applications are expected to exploit the unique chemistry and advantages associated with this surface modification strategy. Here, strategies that rely on the covalent incorporation of additional components, such as polymers, are expected to feature prominently. Even if the AMN-based coatings are obtained from cyano-containing molecules their cytotoxicity is extremely low, which highlights the possibility to produce biocompatible materials from known toxic building blocks. However, the long-term stability and the influence of degradation products of the AMN-based coatings needs to be thoroughly investigated.

Author Contributions: H.T.: Conceptualization and methodology. R.A.E.: Conceptualization and formal analysis. V.B.: writing-original draft preparation and investigation. All authors have read and agreed to the published version of the manuscript.

Funding: This research received no external funding.

Conflicts of Interest: The authors declare no conflict of interest.

References

1. Crick, F.H.; Orgel, L.E. Directed panspermia. *Icarus* **1973**, *19*, 341–348. [[CrossRef](#)]
2. Miller, S.L. A production of amino acids under possible primitive earth conditions. *Science* **1953**, *117*, 528–529. [[CrossRef](#)] [[PubMed](#)]
3. Bada, J.L. New insights into prebiotic chemistry from Stanley Miller's spark discharge experiments. *Chem. Soc. Rev.* **2013**, *42*, 2186–2196. [[CrossRef](#)] [[PubMed](#)]
4. Moser, R.E.; Claggett, A.R.; Matthews, C.N. Peptide formation from aminomalononitrile (HCN trimer). *Tetrahedron Lett.* **1968**, *13*, 1605–1608. [[CrossRef](#)]
5. Raulin, F.; Fonsalas, F.; Wolny, M. Aminomalonitrile: Some new data of prebiotic interest. *Orig. Life* **1984**, *14*, 151–156. [[CrossRef](#)]
6. Ferris, J.P.; Hagan, W.J. HCN and chemical evolution: The possible role of cyano compounds in prebiotic synthesis. *Tetrahedron* **1984**, *40*, 1093–1120. [[CrossRef](#)]
7. Ruiz-Bermejo, M.; Zorzano, M.-P.; Osuna-Esteban, S. Simple organics and biomonomers identified in HCN polymers. *Life* **2013**, *3*, 421–448. [[CrossRef](#)]
8. Villafaña-Barajas, S.A.; Ruiz-Bermejo, M.; Rayo-Pizarosso, P.; Colin-Garcia, M. Characterization of HCN-derived thermal polymer: Implications for chemical evolution. *Processes* **2020**, *8*, 968. [[CrossRef](#)]
9. Matthews, C.N.; Minard, R.D. Hydrogen cyanide polymers, comets and the origin of life. *Faraday Discuss.* **2006**, *133*, 393–401. [[CrossRef](#)]

10. D'Ischia, M.; Manini, P.; Moracci, M.; Saladino, R.; Ball, V.; Thissen, H.; Evans, R.A.; Puzzarini, C.; Barone, V. Astrochemistry and astrobiology: Materials science in Wonderland? *Int. J. Mol. Sci.* **2019**, *20*, 4079.
11. Thissen, H.; Kogler, A.; Salwiczek, M.; Easton, C.D.; Qu, Y.; Lithgow, T.; Evans, R.A. Prebiotic-chemistry inspired polymer coatings for biomedical and material science applications. *NPG Asia Mater.* **2015**, *7*, e225. [[CrossRef](#)]
12. Toh, R.J.; Evans, R.; Thissen, H.; Voelcker, N.H.; d'Ischia, M.; Ball, V. Deposition of aminomalononitrile-based films: Kinetics, chemistry, and morphology. *Langmuir* **2019**, *35*, 9896–9903. [[CrossRef](#)] [[PubMed](#)]
13. Menzies, D.J.; Ang, A.; Thissen, H.; Evans, R.A. Adhesive prebiotic chemistry inspired coatings for bone contacting applications. *ACS Biomater. Sci. Eng.* **2017**, *3*, 793–806. [[CrossRef](#)]
14. Ball, V. Anti-oxidant activity of films inspired by prebiotic chemistry. *Mater. Lett.* **2020**, accepted.
15. Ruiz-Bermejo, M.; de la Fuente, J.L.; Carretero-González, J.; García-Fernández, L.; Aguilar, M.R. A comparative study on HCN polymers synthesized by polymerization of NH_4CN or diaminomaleonitrile in aqueous media: New perspectives for prebiotic chemistry and materials science. *Chem. Eur. J.* **2019**, *25*, 11437–11455. [[CrossRef](#)] [[PubMed](#)]
16. Ball, V.; Toh, R.J.; Voelcker, N.H.; Thissen, H.; Evans, R.A. Electrochemical deposition of aminomalononitrile based films. *Colloids Surf. A Physicochem. Eng. Asp.* **2018**, *552*, 124–129. [[CrossRef](#)]
17. Jung, J.; Menzies, D.J.; Thissen, H.; Easton, C.D.; Evans, R.A.; Henry, R.; Deletic, A.; McCarthy, D.T. New prebiotic chemistry inspired filter media for storm water/greywater disinfection. *J. Hazard. Mater.* **2019**, *378*, 120749. [[CrossRef](#)]
18. Chen, W.-H.; Liao, T.-Y.; Thissen, H.; Tsai, W.-B. One-step aminomalononitrile-based coatings containing zwitterionic copolymers for the reduction of biofouling and the foreign body response. *ACS Biomater. Sci. Eng.* **2019**, *5*, 6454–6462. [[CrossRef](#)]
19. Liao, T.-Y.; Easton, C.D.; Thissen, H.; Tsai, W.-B. Aminomalononitrile-assisted multifunctional antibacterial coatings. *ACS Biomater. Sci. Eng.* **2020**, *6*, 3349–3360. [[CrossRef](#)]
20. Lee, H.; Dellatore, S.M.; Miller, W.M.; Messersmith, P.B. Mussel inspired surface chemistry for multifunctional coatings. *Science* **2007**, *318*, 426–430. [[CrossRef](#)]
21. Sileika, T.S.; Barrett, D.G.; Zhang, R.; Lau, K.F.A.; Messersmith, P.B. Colorless multifunctional coatings inspired by polyphenols found in tea, chocolate, and wine. *Angew. Chem. Int. Ed.* **2013**, *52*, 10766–10770. [[CrossRef](#)] [[PubMed](#)]
22. Ponzio, F.; Barthès, J.; Bour, J.; Michel, M.; Bertani, P.; Hemmerlé, J.; d'Ischia, M.; Ball, V. Oxidant control of polydopamine surface chemistry in acids: A mechanism-based entry to superhydrophilic-superoleophobic coatings. *Chem. Mater.* **2016**, *28*, 4697–4705. [[CrossRef](#)]
23. Ponzio, F.; Payamyar, P.; Schneider, A.; Winterhalter, M.; Bour, J.; Addigo, F.; Krafft, M.-P.; Hemmerle, J.; Ball, V. Polydopamine films from the forgotten air/water interface. *J. Phys. Chem. Lett.* **2014**, *5*, 3436–3440. [[CrossRef](#)] [[PubMed](#)]
24. Bernsmann, F.; Voegel, J.-C.; Ball, V. Different synthesis methods allow to tune the permeability and permselectivity of dopamine-melanin films to electrochemical probes. *Electrochim. Acta* **2011**, *56*, 3914–3919. [[CrossRef](#)]